The water vapor self-continuum absorption in the infrared atmospheric windows: New laser measurements near 3.3 µm and 2.0 µm

Loic Lechevallier[1,2], Semen Vasilchenko[1,3], Roberto Grilli[2], Didier Mondelain[1], Daniele Romanini[1] and Alain Campargue[1]

[1] Univ. Grenoble Alpes, CNRS, LIPhy, 38000 Grenoble, France
[2] Univ. Grenoble Alpes, CNRS, IRD, Grenoble INP*, IGE, F-38000 Grenoble, France[1]
[3] Laboratory of Molecular Spectroscopy, V.E. Zuev Institute of Atmospheric Optics, SB, Russian Academy of Science, 1 Akademician Zuev square, 634021 Tomsk, Russia

Correspondence to: Alain Campargue (Alain.Campargue@univ-grenoble-alpes.fr)

Abstract. The amplitude, the temperature dependence, and the physical origin of the water vapor absorption continuum are a long-standing issue in molecular spectroscopy with direct impact in atmospheric and planetary sciences. In recent years, we have determined the self-continuum absorption of water vapor at different spectral points of the atmospheric windows at 4.0, 2.1, 1.6 and 1.25 µm, by highly sensitive cavity-enhanced laser techniques. These accurate experimental constraints have been used to adjust the last version (3.2) of the semi-empirical MT_CKD model (Mlawer-Tobin_Clough-Kneizys-Davies) which is widely incorporated in atmospheric radiative-transfer codes. In the present work, the self-continuum cross-sections, C_S, are newly determined at 3.3 µm (3007 cm^{-1}) and 2.0 µm (5000 cm^{-1}) by optical-feedback-cavity enhanced absorption spectroscopy (OFCEAS) and cavity ring-down spectroscopy (CRDS), respectively. These new data allow extending the spectral coverage of the 4.0 and 2.1 µm windows, respectively, and testing the recently released 3.2 version of the MT_CKD continuum. By considering high temperature literature data together with our data, the temperature dependence of the self-continuum is also obtained.

[1]Institute of Engineering Univ. Grenoble Alpes

1. Introduction

About 60% of the solar radiation absorbed by the Earth's atmosphere is due to water vapor absorption. Water vapor absorption involves two contributions*: (i)* a succession of vibrational bands separated by about 1500-2000 cm^{-1} with decreasing intensity from the far infrared to the visible. These are formed by multitudes of narrow rovibrational absorption lines that are tabulated in spectroscopic databases like HITRAN (Gordon et al., 2017) and GEISA (Jacquinet-Hussonet al., 2016), *(ii)* a weak broadband absorption continuum with slow frequency dependence roughly following the contour of vibrational bands. In the regions of low absorption between the vibrational bands - the water vapor transparency windows - the continuum has a major contribution and may dominate the cumulative effect of the weak rovibrational lines. In the Earth's atmosphere, the continuum decomposes into a self-continuum component due to water-water molecular interactions and a foreign-continuum component due to water-nitrogen and water-oxygen interactions. The water self-continuum increases quadratically with the water number density and has strong negative temperature dependence. More than one century after its discovery (Rubens and E. Aschkinass, 1898) and decades of controversy (Shine et al., 2012), the origin of the water continuum remains an open question. The reader is referred to (Camy-Peyret et al., 2003; Ma et al., 2008; Ptashnik et al., 2008, 2011b; Leforestier et al., 2010, Tretyakov et al., 2014; Vigasin, 2014; Buryak and Vigasin, 2015; Serov et al. 2017) for discussions about the respective contributions of the far wings of the rovibrational lines, the water dimers (stable and metastable) and collision-induced absorption.

The water vapor continuum implemented in atmospheric radiative transfer codes is usually the semi-empirical MT_CKD model (Mlawer-Tobin_Clough-Kneizys-Davies) (Clough et al. 1989; Mlawer et al. 2012) which is regularly updated. This model which is basically a far-wing line shape model in the window regions, involves a number of *ad-hoc* parameters that have been constrained to laboratory and field measurements mostly in the far- and mid-infrared. Because of the experimental difficulty in detecting very small variation of the spectrum baseline induced by the injection of water vapor in an absorption cell, up to recently, laboratory measurements were very scarce in the mid- and near-infrared and the MT_CKD model used long range extrapolations with a few experimental constraints dating back to the 1980s (e.g. Burch et al., 1982, 1984, 1985). Thus, a validation of the amplitude and of the temperature-dependence of the MT_CKD continuum in those spectral ranges is highly desirable not only to quantify its impact on the estimated radiative budget of the Earth (Held and Soden, 2000; Ptashnik et al., 2011a; Paynter and Ramaswamy, 2011; 2012; 2014) but also on the extension of the habitable zone around stars (Kastinget al., 1993; Kopparapu et al., 2009; Leconte et al. 2013a; 2013b).

In the last decade, experimental efforts have been undertaken in different laboratories to improve the knowledge of the water continuum in the transparency windows. As a result, coinciding measurements obtained by Fourier Transform Spectroscopy (FTS) with long path absorption cells (Paynter et al., 2009; Ptashnik et al., 2011a; 2013; 2015) were found in strong

disagreement with the MT_CKDV2.5 modeling in the 4.0, 2.1 and 1.6 µm windows. In particular, the reported FTS values are larger by one and two orders of magnitude in the center of the 2.1 and 1.6 µm windows, respectively.

More recently, we have implemented highly sensitive cavity enhanced laser techniques at different spectral points of the 4.0, 2.1, 1.6 and 1.25 µm windows to measure in the laboratory the self-continuum absorption of water vapor (Mondelain et al. 2013; 2014, 2015; Campargue et al. 2016; Ventrillard et al. 2015; Richard et al. 2017). Overall, these measurements by Optical Feedback Cavity Enhanced Absorption Spectroscopy (OFCEAS) and Cavity Ring-down Spectroscopy (CRDS) were found closer to the MT_CKD model than to the FTS results. Experimentally, such investigations are demanding since the tunability of laser sources is generally limited notably in the mid-infrared range, in contrast to FTS which allows for large spectral coverage. Thus each spectral point requires dedicated experimental developments. Nevertheless, the sensitivity, baseline stability and data acquisition speed provided by CRDS and OFCEAS are critical advantages to avoid experimental biases and retrieve accurate continua. In all our previous measurements and contrary to the above mentioned FTS studies, the pressure-squared dependence of the continuum was carefully checked during pressure ramps to insure the gas phase origin of the measured signals and exclude experimental biases related to the stability of the spectrometer or to the impact of water layers or water adsorption on the mirror reflectivity.

In the present work, we report two new measurement points by OFCEAS at 3.33 µm (3007 cm^{-1}) and CRDS at 2.0 µm (5000 cm^{-1}). These measurements complete the sampling of the 4.0 µm and 2.1 µm windows at high energy. In addition, the temperature dependence at 3.33 µm is studied in the 298-323 K interval and discussed in relation with literature data taken at higher temperature. The present results are compared to the recently released 3.2 version of the MT_CKD model which was adjusted taking into account our previous measurements.

The two next sections present, for each of spectral points, the experimental setups, spectra acquired, the continuum retrieval, and a comparison with literature data. Considerations on the temperature dependence are presented in Section 4. A review of the experimental results and of the MT_CKD model in the 1500-9000 cm^{-1} range is presented in the last section.

2. OFCEAS at 3007 cm^{-1}

OFCEAS is a cavity enhanced absorption method alternative to CRDS (Morville et al., 2004; Romanini et al., 2006; Maisons et al., 2010; Gagliardi and Loock, 2014) which has specific advantages, in particular for trace analysis (Kassi et al. 2006; Faïn et al. 2014; Desbois et al. 2014). This technique uses feedback of light from a high-finesse V-cavity to lock the laser emission over cavity resonances during a laser frequency scan. Every second, several spectra over a small spectral interval (~ 1 cm^{-1}) are obtained allowing for an efficient statistical averaging. While CRDS relies on the measurements of the lifetime of the photons in the cavity, OFCEAS provides transmission spectra. Using the photon lifetime measured at the end of each scan, the cavity transmission is converted into a spectrum in absolute absorption coefficient scale using the procedure detailed in Kerstel et al. (2006) and Richard et al. (2017).

2.1 Spectra acquisition

The OFCEAS spectrometer used in this work is similar to that presented in Ventrillard et al., (2015) and Richard et al. (2017). The laser source (from Nanoplus GmbH) is an Interband Cascade Laser (ICL) emitting between 3005.5 and 3009.5 cm^{-1} by acting on its operating current and temperature. The cavity mirrors (from LohnStar Optics) have a 99.96 % reflectivity as deduced from a measured ring-down time of 3.20 µs with empty cavity. The acquired spectra have an intrinsically linear frequency scale with equally spaced spectral points separated by the cavity Free Spectral Range, $FSR=c/2nL$, where c is the speed of light, L the effective cavity length, and n the refractive index of the intra-cavity sample. Both arms of the V-cavity have a length of 40 cm leading to an *FSR* of 187.4±0.5 MHz. A spectrum over 105 cavity modes (or *FSR*) corresponding 0.7 cm^{-1} is acquired within about 100 ms by modulation of the laser current at 10 Hz. The laser current scans and operating temperature, the cavity temperature and pressure, and data acquisition as well, were controlled by an electronic card (from AP2E). The optical assembly is composed by the diode laser, an infrared polarizer (colorPol MIR), two stirring aluminum mirrors, two photodiodes (PCI-2TE-4), and the optical cavity (7.75 mm apex diameter). This is made of out of a stainless-steel single piece which contains a V-shaped (6 mm diameter) channel with gas inlet and outlet for the sample flow, and also carries the three high reflectivity mirrors permanently aligned on removable vacuum-tight metal holders. The laser ramp is provided by the software, and the frequency acquisition rate is maximized. The whole assembly is suspended on two anti-vibration mounts, and confined in a thermal isolated aluminum case. A Pt1000 thermistance is placed at the center of the cavity and its temperature is controlled by heating bands *via* a PID regulation. In this study, the temperature of the high finesse cell was varied between 25 °C and 50 °C. Water vapor was generated by using a steel tank filled with few cm^3 of deionized water connected to the spectrometer upstream. Series of spectra were recorded in a flow regime (typically 0.13 sccm) during pressure ramps up to 23 mbar, in order to remain below the saturation pressure (about 28 mbar at 296 K).

The pressure ramp was adjusted by a manual valve and a proportional computer-controlled electro-valve placed before and after the cavity, respectively. About 6000 spectra were recorded during the pressure ramp (about 10 min). The gas pressure was measured upstream of the cavity by a high accuracy CPG2500 pressure gauge (from Mensor, 0-1000 mbar with an accuracy better than 0.5 mbar). A second sensor was directly connected to the cavity. During the data acquisition, we noted significant differences between the pressure values provided by the two sensors, especially for low pressure values indicating the presence of a pressure gradient and different Venturi depression between the two measurement points. These pressure artefacts depend on the configuration of gas lines and can become significant when pressure is low and rapidly varying. At the end, we decided to deduce the actual water vapor pressure (or molecular density) by directly using two relatively strong absorption lines of the main water isotope ($H_2{}^{16}O$) present in the recorded spectra (see below).

The calibration of the frequency axis relies on the known *FSR* value (187.5 MHz) and on the absolute frequency of water absorption lines as given in theHITRAN2016 database (Gordon et al., 2017). **Fig. 1** shows typical spectra obtained with the OFCEAS system for a temperature of 50°C and pressure of 5, 15 and 20 mbar. The increase of the baseline level and of the absorption lines with pressure is clearly apparent. The baseline is not completely flat because of optical interference pattern

which is produced between the output cavity mirror and the photodiode. Several efforts have been made in order to minimize these effects, but it was not possible to remove them completely. However, these optical fringes are taken into account in the spectral fit and therefore removed for the spectral analysis.

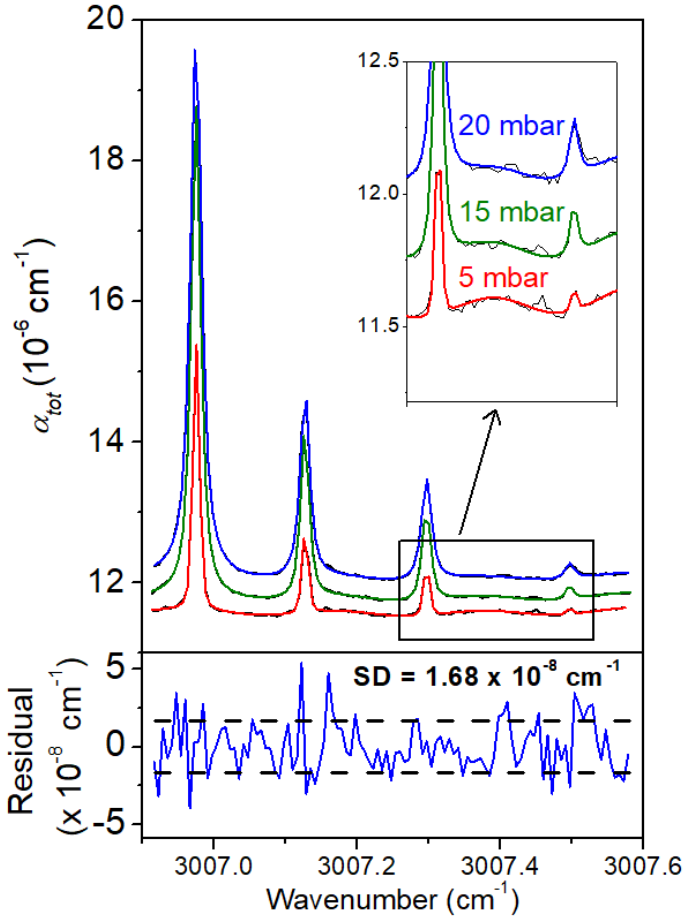

Figure 1: *Upper panel:* Total absorption coefficient measured by OFCEAS when the optical cavity is filled by water at three different pressures for a temperature of 50 °C. Black lines are experimental data while colored lines the corresponding spectral fits, as described in the text.
Lower panel: Residuals of the fit for the spectrum at 20 mbar.

2.2. Self-continuum cross-section retrieval

The OFCEAS absorption coefficient is the sum of the contribution of the losses of the (evacuated) cavity, α_{cavity}, and of water absorption. The latter includes water vapor monomer local absorption lines (WML) and water vapor self-continuum (WCS):

$$\alpha_{tot}(\nu,T) = \alpha_{cavity}(\nu) + \alpha_{WML}(\nu,T) + \alpha_{WCS}(\nu,T) \quad (1)$$

Note that Rayleigh scattering contribution is negligible (Thalman et al., 2014).

It is worth noting that α_{WML} accounts not only for the four water lines observed in the spectra (**Fig. 1**) but also for the contribution of the wings of the lines located outside the recorded region. As the recorded spectral interval corresponds to a micro window surrounded by lines with intensity up to 4-5 orders of magnitude larger than those observed in **Fig. 1**, the monomer wing contribution in this region is in fact the dominant contribution to the baseline increase. According to the usual definition of the water continuum, lines located in the [ν-25, ν+25 cm^{-1}] wavenumber interval have to be considered and simulated using the HITRAN2016 database with a Voigt profile truncated at ±25 cm^{-1} from the line center. Note that similarly to the continuum, the monomer wing contribution has quadratic pressure dependence.

For each spectrum, the baseline is determined by effectively subtracting the four absorption lines using a spectral fit procedure. A Rautian profile was used to fit the line profile by fixing the Doppler widths to the theoretical values and adjusting the Lorentzian collisional broadening and Dicke narrowing for each individual absorption line. The baseline is fitted by a third order polynomial in the basis of Legendre Gauss polynomials. Optical fringes due to parasite reflections are taken into account by adding three sine waves at fixed frequency and amplitude with free phase (frequencies and amplitudes were determined by FFT analysis of the fit residuals before inclusion of these terms). The quality of the spectrum simulation is illustrated by the residuals displayed in the bottom panel of **Fig. 1**, showing an *rms* of the residuals of 1.7×10^{-8} cm^{-1} at 20 mbar for a single scan (100 ms). As mentioned above, the pressure value of each spectrum was calculated using the water absorption lines. The integrated absorption coefficient of a given line is simply the product of the molecular density (in $molecule.cm^{-3}$) by the line intensity (in cm/molecule) as tabulated in the HITRAN2016 database. In the studied interval, the two strongest lines at 3006.975 and 3007.1278 cm^{-1} are due to the main isotopologue ($H_2{}^{16}O$). Their intensities were recently measured by Loos et al. (2017) with an accuracy of 1.5 % and 2.4 %, respectively. As a validation test, we present in **Fig. 2** the ratios of the pressure values derived from these two lines during a pressure ramp at 50 °C. The small dispersion of the ratio values along the ramp confirms the stability of the experiment (average value of 1.056 with a standard deviation of 1.0 %). Considering all the ramps recorded at different temperatures, we obtain an average ratio of 1.041 and a standard deviation of 0.84 %, which is consistent with the intensity error bars reported by Loos et al. (2017). Note that compared to Loos et al. (2017), the *ab initio* values of the BT2 (Barber et al., 2006) and Schwenke and Partridge (2000) theoretical databases of water vapor transitions gives ratio of 1.048 and 1.061, respectively. As a result, the pressure of each spectrum was obtained as the average value of the two determinations with an associated error bar estimated to 3 %.

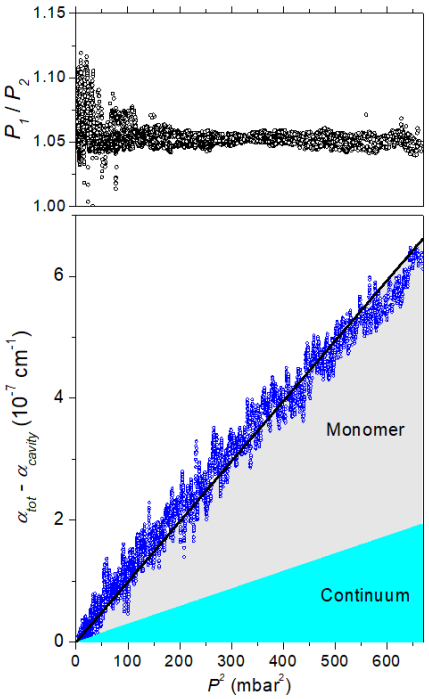

Figure 2: *Upper panel:* Ratio of the pressure values deduced from the $H_2{}^{16}O$ line at 3006.975 cm^{-1} (P_1) and at 3007.127 cm^{-1} (P_2) as a function of P_1 for a pressure ramp at 50 °C.
Lower panel: Corresponding variation of the water continuum absorption near 3007 cm^{-1} as a function of pressure squared. The plotted data correspond to the superposition of 5 distinct pressure ramps smoothed over ten adjacent measurements points. The solid black line corresponds to the best linear fit. The constant term due to the cavity losses obtained from the fit was subtracted. The simulated contribution of water monomer wings and that of the self-continuum are highlighted (in grey and cyan, respectively).

Fig.2 presents the dependence of the zero order term of the baseline fit *versus* the squared pressure, during a pressure ramp at 50°C. A convincing quadratic dependence is obtained. After subtraction of the constant term due to the cavity losses, the plotted quantity results as the sum of the water vapor continuum (α_{WCS}) and the monomer wing contributions, which have both a quadratic pressure dependence. Let us note that the wing contribution, calculated as indicated above, is more than twice the water vapor continuum. The large number of scans performed for each pressure ramp (typically, 6000 spectra per ramp of 10 min duration) allows increasing the precision of the fitted value of the quadratic coefficient, $\alpha_{WCS}(\nu,T)/P^2$ which defines the self-continuum cross-section, C_S, (in cm^2 molecule^{-1} atm^{-1}): $\alpha_{WCS}(\nu,T) = \frac{1}{k_B T} C_S(\nu,T) P^2$, where k_B is the Boltzmann constant. The obtained C_S values are listed in **Table 1** for six temperature values ranging from 25 °C to 50 °C

Table 1.

Self-continuum absorption cross-sections of water vapor measured near 3007 and 5000 cm^{-1}

Wavenumber (cm^{-1})	*T(K)*	*C_S (10^{-23} cm^2 $molecule^{-1}$ atm^{-1})*
3007	298.15	1.96(39)
	303.15	2.17(54)
	308.15	1.83(46)
	313.15	1.43(36)
	318.15	1.82(46)
	323.15	1.40(35)
4995.63	297.82	0.757(38)
4998.98	297.48	0.776(39)
5002.05	297.80	0.798(40)
5006.67	297.32	0.794(40)

Note

Numbers in parenthesis correspond to the 1-σ overall estimated error bars in units of the last quoted digit.

In the present case, the error bars on C_s values are relatively large, on the order of 25 %. This results from different factors. The statistical error bars of the fitted value of the quadratic coefficient is on the order of 4 %, mainly due to fluctuations of the spectra baseline level related to the short ring down time provided by the cavity mirrors. Taking into account that the water continuum represents about 28 % of the measured signal (**Fig. 2**), this fit error gives a 15-20 % relative uncertainty on C_s. The uncertainty on the pressure values derived from the absorption lines contributes also to the error budget (see above). It results from the uncertainty on the intensity values reported by Loos et al. (2017) and from the ±1 K uncertainty on the gas temperature that affects line intensities (the two water lines have a relatively high lower state energy -1813.8 and 1394.8 cm^{-1} - leading to a strong temperature dependence of their intensities i.e. 2.3% per K for the strongest line). In Richard et al. (2017), a pressure ramp of dry nitrogen up to 40 mbar was performed, proving that the optical signal is not sensitive to pressure changes. Thus the cavity instability is not expected to contribute significantly to the error budget. Overall, we estimate the 1-σ error bar of the C_S values to be 20 % for the room temperature value (298 K) and 25 % at higher temperature.

In the present situation where the measured continuum signal is dominated by the water monomer contribution, the retrieved C_S values are strongly dependent on the quality of the monomer line parameters, in particular the self line width broadening coefficient. Following the standard approach the uncertainty in line parameters of neighboring strong lines was not incorporated in our overall error bar. Our C_S values should then be associated to HITRAN2016 line parameters of water vapor to account for the overall absorption of water vapor in this region. Let us mention that most of the monomer contribution near 3007 cm^{-1} is due to three very strong lines at 3004.686, 3005.454 and 3010.232 cm^{-1} with line intensities in the 8×10^{-23}-7×10^{-22} cm/molecule range. HITRAN2016 line list of water vapor reproduces the line parameters obtained by

Loos et al. (2017) in this region. For these three strong lines, Loos et al. reported an error bar of less than 0.8 % for the self broadening parameters. This is significantly lower than the 20-25 % error bar on the reported C_S values.

2.3. Comparison to literature

The different experimental determinations of the self-continuum cross-sections at room temperature in the 4 µm window are gathered in **Fig. 3** together with some of the last versions of the MT_CKD continuum up to the current 3.2 version. In addition to the present study at 3007 cm^{-1} located at the high energy edge of the window, previous OFCEAS studies were performed at 2283cm^{-1} (Campargue et al., 2016) and 2491 cm^{-1} (Richard et al., 2017). Three datasets were obtained by FTS with long-path absorption cells and cover most of the transparency window: *(i)* CAVIAR consortium dataset obtained with a 512.7 m pathlength at 293 K (Ptashnik et al., 2011a), *(ii)* two series of FTS determinations from IAO in Tomsk (Ptashnik et al., 2013; 2015), obtained with a pathlength of 612 m at 289.5 and 287 K, respectively, *(iii)* the FTS dataset obtained at NIST by Baranov and Lafferty (2011) with a 100 m pathlength between 311 and 363 K. Finally, Burch and Alt (1984) reported continuum measurements in the center of the window using a grating spectrograph and an optical configuration aiming to minimize the spectra baseline drifts.

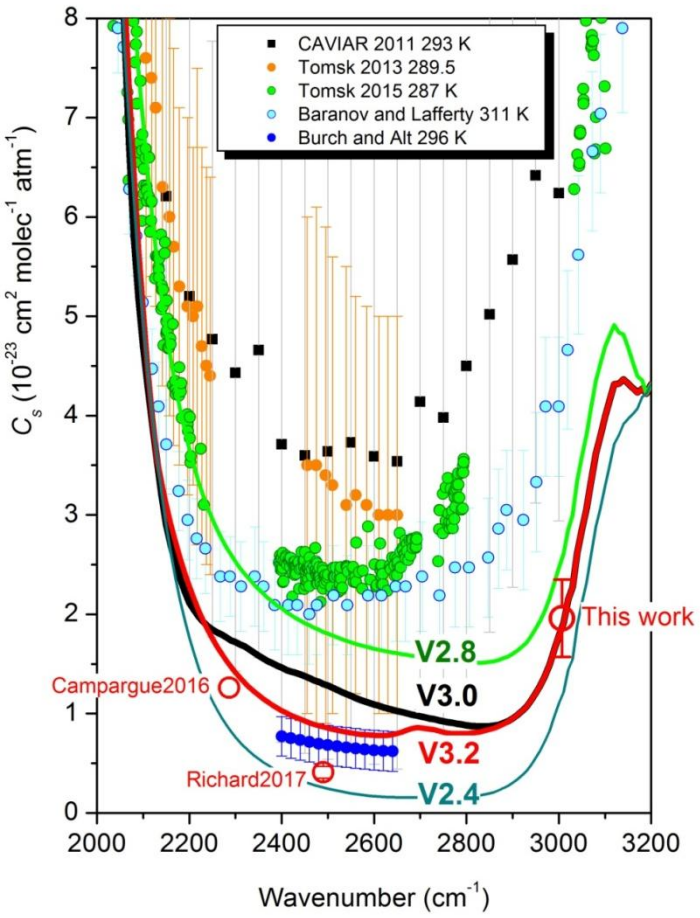

Figure 3: Overview comparison of the self-continuum cross-section of water vapor near room temperature. Solid lines show different versions of the MT_CKD model at 296 K. Experimental results are obtained using different techniques, namely by OFCEAS, (red circles; Campargue et al., 2016; Richard et al., 2017; this work); by FTS from Baranov and Lafferty (2011), light blue circles, from CAVIAR (black squares; Ptashnik et al., 2011a), from Tomsk2013 (orange circles; Ptashnik et al., 2013), from Tomsk2015 (green circles; Ptashnik et al., 2015) and with a grating spectrograph by Burch and Alt (1984), dark blue circles. Note that the plotted experimental results correspond to different temperature values (see temperature values given in the insert). The temperature of the OFCEAS results are 296.15, and 297.3 and 298.15 K, for Campargue et al., 2016, Richard et al., 2017 and this work, respectively. The 30-50 % error bars on Tomsk2015 values are omitted for clarity.

At 3007 cm^{-1}, the present OFCEAS and the MT_CKD3.2 values are in excellent agreement. The comparison to the FTS values is similar to that encountered in most of the transparency windows: the FTS values are overestimated compared to both MT_CKD and the laser measurements. The CAVIAR C_S value at 296 K and Tomsk 2015 value at 287 K were reported with a 50 % error bar. A rough extrapolation at 300 K leads to C_S = 6.3 and 4.53×10^{-23} cm^2 molec^{-1} atm^{-1}, respectively which should be compared to an OFCEAS value of 1.96 ×10^{-23} cm^2 molec^{-1} atm^{-1}.at 298 K. The FTS value reported by Baranov and Lafferty at 311 K with a 22% error bar corresponds to about 5.41 ×10^{-23} cm^2 molec^{-1} atm^{-1} at 300 K.

The evolution of the MT_CKD model in the 4.0 µm over the last ten years is illustrated by the 2.4, 2.8, 3.0 and 3.2 versions plotted in **Fig. 3**. In the center of the window, the different versions have varied over one order of magnitude amplitude. On the basis of the OFCEAS measurement at 2283 cm^{-1} (Campargue et al. 2016), the MT_CKD3.2 version of the self-continuum has been recently decreased in the low energy edge of the window. In the high energy edge of the window, the present measurement at 3007 cm^{-1} validates the V3.2 values which are unchanged from V3.0.

3. CRDS near 5000 cm^{-1}

3.1 Spectra acquisition and self-continuum cross-section retrieval

The reader is referred to (Čermáket al., 2016; Campargue et al. 2017) for a description of our CRDS spectrometer dedicated to the high sensitivity spectroscopy of atmospheric species in the 2.1 µm window. The setup is an improved version of that used for absorption lines and continuum measurements of water vapor (Campargue et al. 2017) and CO_2 (Mondelain et al., 2017) absorption. A Distributed Feed Back (DFB) diode laser (from Eblana Photonics) covering the 4995-5007 cm^{-1} spectral interval was used as light source. The optical feedback technique (Lin et al. 2012) was used to narrow the laser emission line width and increase the light injection into the cavity during resonances with cavity modes. The frequency of the laser diode was measured with a wavelength meter (model 621-A IR from Bristol Instruments, 8 MHz 1-σ accuracy and 2.5 Hz acquisition rate). The present measurement points of the water continuum near 5000 cm^{-1} extend to high energy our OFCEAS and CRDS measurements in the 2.1 µm window.

Fig. 4 shows an overview of the water vapor CRDS spectrum near 5002 cm^{-1} and the location of one of the four spectral points selected for the water vapor absorption continuum retrieval. From the spectrum recorded with an unprecedented sensitivity in the region (α_{min}~ $3\times10^{-10}cm^{-1}$), water vapor transitions with intensity values below 1×10^{-28} cm/molecule are measured. The recorded spectrum was found in very good agreement with simulations performed on the basis of the HITRAN2016 database (see **Fig. 4**).

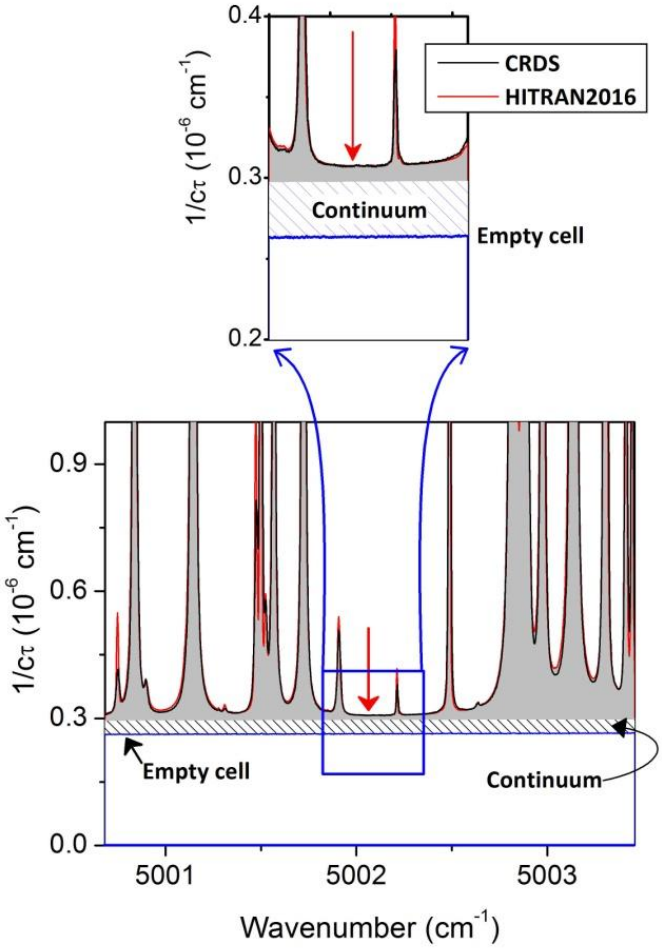

Figure 4: CRDS spectrum of water vapor between 5000.6 and 5003.5 cm^{-1}. The pressure was 7.0 Torr at 297.35 K. The red arrow indicates one of the four spectral points located in an interval free of absorption lines, which was chosen for the retrieval of the water vapor absorption continuum. The simulation performed on the basis of the HITRAN2016 database (red solid line) is used to subtract the monomer contribution. The water continuum (dashed area) corresponds to the gap between the spectrum with the monomer simulation subtracted and the baseline level recorded with the evacuated cell.

The CRDS cell was filled with water vapor after purification by liquid nitrogen cooling and pumping on the residual vapor phase. The pressure in the cell was continuously monitored with a capacitive transducer (model ATM.1ST from STS; 50 mbar full range; accuracy of ±0.1 % of the full range). Contrary to the above OFCEAS measurements, for which the self-continuum was derived from a series of spectra, the present CRDS measurement were performed at fixed frequency by monitoring the variation of the cavity loss rate, $1/c\tau$, during pressure ramps. The typical value of the ring-down time of the evacuated cavity, τ_0, was about 124 µs and the acquisition rate was about 60 ring-down events per second. About 8000 ring-down events were measured during upward and downward pressure ramps up to 15 Torr, at four selected spectral points free of absorption lines (see **Table 1**). The typical duration of the ramps was 90 s and the cell temperature was about 297.5 K.

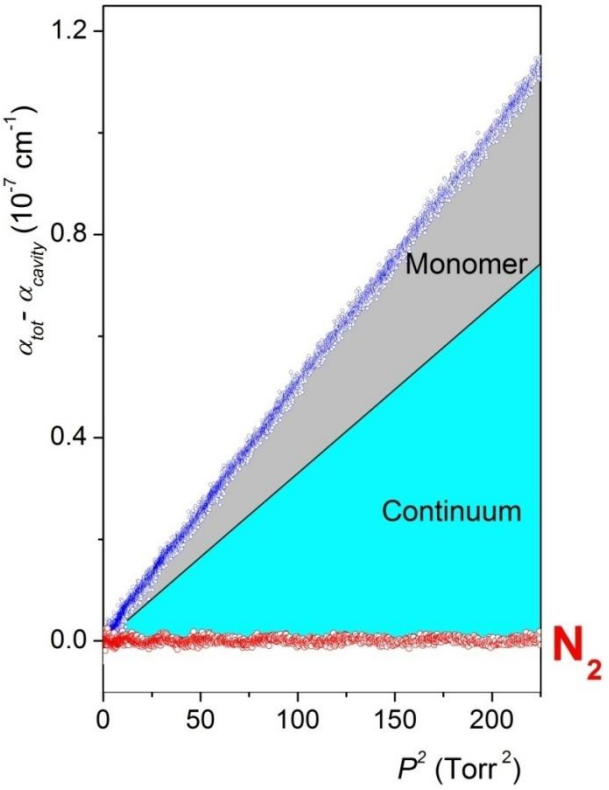

Figure 5: Variation of the loss rate measured by CRDS at 4995.63 cm^{-1} during the filling of the cell with water vapor up to 15 Torr. The constant term due to the cavity losses obtained from the fit was subtracted. Every blue dot corresponds to a single ring-down event. Red dots represent similar measurements performed with pure nitrogen. The simulated contribution of water monomer and the self-continuum are highlighted in grey and cyan, respectively.

Fig. 5 shows the variation of the loss rate at 4995.63 cm^{-1} during the filling of the CRDS cell. No deviation from the quadratic law is noted up to the maximum pressure value of 15 Torr corresponding to 65 % humidity rate. The loss rate is the sum of the loss rate with the cell evacuated and of the absorption coefficient, $\alpha(\nu)$, due to water vapor:

$$\frac{1}{c\tau(\nu)} = \frac{1}{c\tau_0(\nu)} + \alpha(\nu) \qquad (2)$$

where c is the speed of light. The Rayleigh scattering contribution being negligible, the absorption coefficient includes contributions due to water vapor monomer local lines (WML) and water vapor self-continuum (WCS). The water absorption continuum was then obtained after subtraction of the WML contribution calculated as indicated above. According to the spectral points, the WML contribution represents between 18 and 38 % of the total absorption (38 % at 4995.63 cm^{-1} as illustrated in **Fig. 5**). The self-continuum absorption cross-sections included in **Table 1** were derived from the linear fit of the absorption continuum in *P*-squared. As a result of the large number of measurements for each pressure ramp and of the very good mechanical stability of the cavity, the statistical error on the fitted coefficient is very small, less than 1 %. The

mechanical and optical stability of the spectrometer was checked by using nitrogen (N_2) instead of water vapor. The results included in **Fig. 5**confirm that the measurements are not affected by the pressure variation during the pressure ramp.

The C_S values listed in **Table 1** are values averaged for an upward and downward pressure ramps. Maximum differences of less than 2 % were obtained between upward and downward determinations. Taking into account other error sources (0.25 % on the pressure measurements, 0.2 °C on the temperature, fit error), we estimate to less than 5 % the relative uncertainty on the listed $C_S$values.

3.2. Comparison to literature

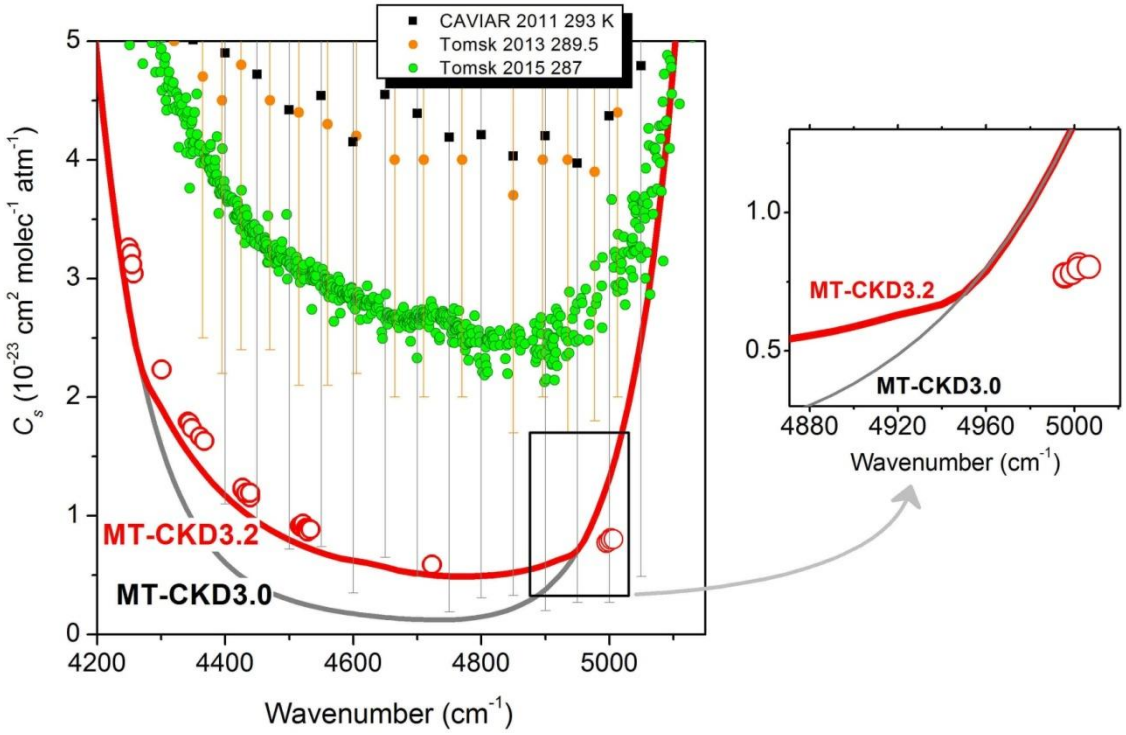

Figure 6: Spectral dependence of self-continuum cross-section at room temperature in the 2.1 µm window. The two last versions of the MT_CKD model (V3.0 and V3.2, black and red solid lines, respectively) are compared to the cavity-based measurements (red circles), to the FTS results obtained in Tomsk (Ptashnik et al., 2013, 2015; green and orange circles) or by the CAVIAR consortium (Ptashnik et al., 2011a) (black squares). The 30-50 % error bars on the Tomsk2015 FTS values and the small error bars on our laser based values are not plotted for clarity. The zoom highlights the present CRDS values near 5000 cm^{-1}.

Although the four spectral points presently selected span less than 12 cm^{-1}, a significant increase is observed with the frequency for the self-continuum cross-sections presented in the inset of **Fig. 6. Fig. 6** shows an overview comparison of previous FTS and laser based measurements in the 2.1 µm window with the 3.0 and 3.2 versions of the MT_CKD model. On the basis of our preceding CRDS and OFCEAS measurements below 4750 cm^{-1}, the very recent 3.2 version was significantly increased in the 4250-4950 cm^{-1} range. Above this value, the 3.0 version was kept unchanged. The present C_S values near

5000 cm^{-1} are fully consistent with our previous results and on line with a linear extrapolation of the V3.2 model above 4950 cm^{-1}. It indicates that the present MT_CKD spectral dependence is validated up to 4950 cm^{-1} but should be decreased by about a factor of 2 at 5000 cm^{-1}. Similarly to the situation found in the 4.0 µm, the FTS values of the CAVIAR consortium and of the two Tomsk datasets are largely overestimated, by about a factor of 5 in the present case. In our opinion, as the three sets of FTS values are reported with very large error bars (up to ±94 % for the CAVIAR value), they should be considered as upper limit values corresponding to the detectivity threshold of the FTS setups.

4. Temperature dependence

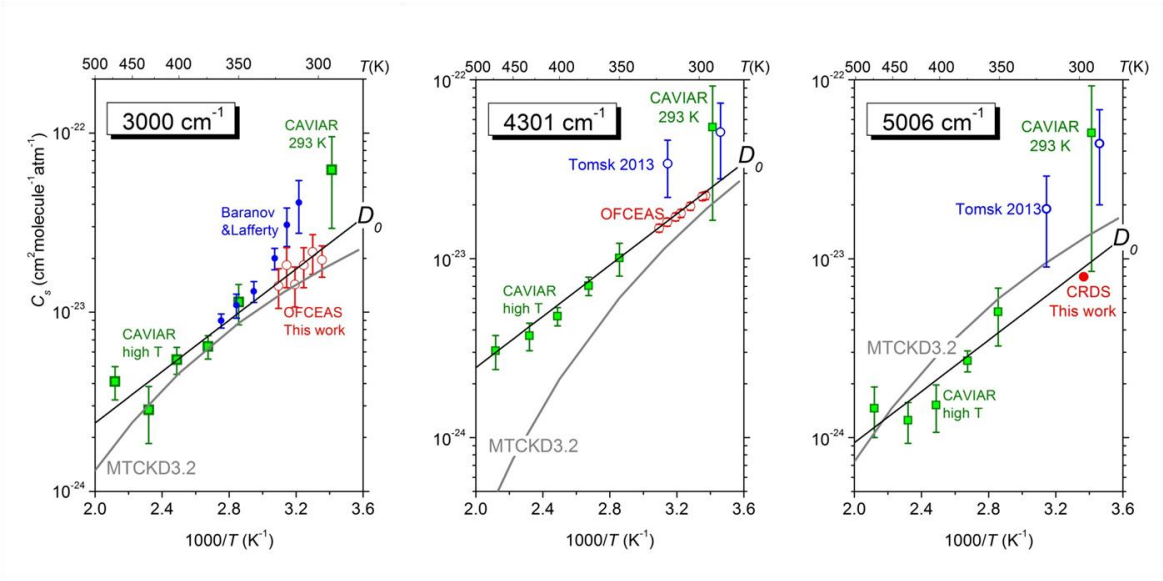

Figure 7: Temperature dependence of the water vapor self-continuum cross-sections near 3000, 4301 and 5006 cm^{-1} obtained by OFCEAS and CRDS (open and full red circles, respectively), by FTS (green squares: CAVIAR; full blue circles: Baranov and Lafferty (2011); open blue squares: Tomsk 2013). The MT_CKD3.2 values which are normalized to the number density at 1 atm and 296 K were multiplied by 296/*T*. The D_0 slope corresponds to an exp(D_0/*kT*) function, $D_0 \approx 1100$ cm^{-1} being the dissociation energy of the water dimer molecule.

The characterization of the temperature dependence of the water vapor self-continuum is an important issue in particular in the temperature range relevant for atmospheric applications. While the water continuum is stronger at low temperature, it is in fact easier to measure it at high temperature where the pressure limitation due to the saturation pressure is strongly relaxed. We have collected in **Fig. 7,** the self-continuum cross section values provided in the literature at different temperatures around our measurement points at 3007 and 5000 cm^{-1} and plotted them in logarithmic scale *versus* 1/*T*. The present OFCEAS measurements cover the 298-323 K interval and shows a decreasing tendency with temperature. In addition to the room temperature FTS studies discussed above, prior measurements at 3000 cm^{-1} were reported by the CAVIAR consortium at temperatures from 350 to 472 K using a short-path absorption cell and vapor pressure values up to

1.6 atm while Baranov and Lafferty (2011) reported FTS measurements in the 311-363 K range. We have also included in **Fig. 7**, a similar plot for the 4301 cm^{-1} spectral point measured by OFCEAS (Ventrillard et al.; 2015). At 4301 cm^{-1}, the whole set of measurements follows a simple exponential law in $1/T$ with a slope close to the dissociation energy of the water dimer, $D_0 \approx 1100$ cm^{-1} (Rocher-Casterline et al., 2011). The set of measurements at 3000 cm^{-1} is consistent with the same $\exp\left(\frac{D_0}{kT}\right)$ temperature dependence but less convincing as a result of larger error bars on the OFCEAS and CAVIAR high temperature values. The situation is mostly similar at 5006 cm^{-1} where our accurate $C_S$value at room temperature is on line with the high temperature CAVIAR values reported with larger error bars.

Overall, the MT_CKD temperature dependence at 3007 and 5000 cm^{-1} agrees with the available experimental data (see **Fig. 7)**. At 4301 cm^{-1}, the MT_CKD temperature dependence is stronger in particular for high temperature values. Nevertheless, near room temperature, the MT_CKD dependence follows $\exp\left(\frac{D_0}{kT}\right)$ function at the three considered spectral points.

5. Conclusion

Using cavity-enhanced absorption methods, the infrared water vapor continuum has been determined at two new frequencies in the 4.0 and 2.1 µm windows. We present in **Fig. 8** an exhaustive comparison of the experimental self-continuum cross-sections with the MT_CKD3.0 and 3.2 models, from 1500 to 9000 cm^{-1}. As mentioned above, the 3.2 version has been adjusted according to the laser-based results listed in **Table 2**. In the 1.6 and 1.25 µm windows, where the continuum is very weak and where previous experimental results were practically absent, the CRDS measurements were found in an overall good agreement with previous versions of the MT_CKD model and the changes associated with the 3.2 version are small in the center of the windows. The largest correction concerns the low energy edge of the 1.25 µm window near 7500 cm^{-1} where the MT_CKD continuum results smaller by a factor of 3. Surprisingly, more significant corrections concern the 4.0 and 2.1 µm windows which have a larger atmospheric impact. Compared to V3.0, the V3.2 C_S values are smaller by about 40 % near the center of the 4.0 µm window. The present results at 3307 cm^{-1} validate the high energy edge of the 4.0 µm window within a 20 % error bar. Nevertheless, there is a disagreement by a factor of 2 between our recent OFCEAS measurement in the center of the window at 2491 cm^{-1} (Richard et al, 2017) and the V3.2 continuum. The Richard et al. value was considered in developing recent MT_CKD version, but found to not be consistent with the satellite- and ground-based observations analyzed in Mlawer et al. (2012). Therefore MT_CKD values were reduced in the 4.0 µm window to take into account the new measurement from Richard et al. while maintaining the agreement with field observations. Further observations and foreign continuum measurements in the center of the 4.0 µm window will hopefully resolve this issue.

The 2.1 µm window has been sampled by CRDS and OFCEAS at seven spectral intervals. This very consistent set of measurements (**Fig. 6**) leads to a strong increase of the continuum in this window (by a factor of ~ 4 near the center) with respect to the MT_CKD3.0. At the high energy edge, above 4950 cm^{-1}, the V3.2 values are unchanged with respect to the

V3.2 version and overestimate by about a factor of ~2 the present CRDS results near 5000 cm^{-1}. As illustrated in **Fig. 6**, the V3.2 correction should be extended at higher energy resulting in a wider 2.1 µm window.

The strong disagreement with FTS measurements (Ptashnik et al., 2011a, 2013, 2015) has been discussed by Shine et al., 2016 and Campargue et al. 2016. The measurement of a very small variation of a FTS spectrum baseline induced by the injection of water vapor in an absorption cell requires high baseline stability during the entire measurement period. In our opinion, traditional methods such as FTS with absorption pathlengths limited to a few hundred meters do not provide sufficient sensitivity and stability to evaluate sub % baseline variations (For instance, in the center of the 4.0 and 2.1 µm windows, at 15 mbar, the continuum measured by OFCEAS and CRDS and predicted by the MT_CKD model corresponds to a 0.1-0.2 % light attenuation for a 500 m absorption pathlength). As underlined by Burch and Alt (1982, 1984, 1985), experimental biases related to optical or mechanical changes lead generally to overestimated values of the continuum. We believe that the high and mostly constant Tomsk and CAVIAR C_s values of about 4×10^{-23} $cm^2molec^{-1}atm^{-1}$ reported for the 4.0, 2.1 and 1.6 µm windows should be considered as an upper limit due to the detectivity threshold of the FTS approach. As a rule, the retrieval of a very weak water continuum from a single pressure spectrum is hazardous. The pressure-squared dependence of the absorption signal, systematically fulfilled in the CRDS and OFCEAS studies, provides a crucial test to ensure that baseline variation of the spectra has a gas-phase origin. This is an important advantage of the cavity-based approach, to allow monitoring the pressure dependence of the continuum absorption during pressure ramps lasting no more than a few minutes. In addition, using similar pressure ramps with non-absorbing gases (N_2 or Ar), the baseline stability of the laser setups can easily be evaluated: no systematic variations were found at the level of the baseline noise level in the range of pressures employed.

Table 2

Summary of the self-continuum retrievals of water vapor performed by CRDS and OFCEAS

Window Approx. center	Measurement points (cm^{-1})	Method	Laser source [a]	*T* (K)	*Ref.*
2500 cm^{-1} (4.0 µm)	2283	OFCEAS	QCL	296, 301, 312	Campargue et al., 2016
	2491	OFCEAS	ICL	297, 312, 325	Richard et al., 2017
	3007	**OFCEAS**	**ICL**	**298-323**	**This work**
4700 cm^{-1} (2.1 µm)	4249-4257 (4 pts)	CRDS	DFB	298	Mondelain et al., 2015
	4301	OFCEAS	DFB	297-323	Ventrillard et al., 2015
	4341-4367 (5 pts)	CRDS	VECSEL	297	Campargue et al., 2016
	4427-4441 (3 pts)	CRDS	DFB	296	Richard et al., 2017
	4516-4532 (8 pts)	CRDS	DFB	297	Campargue et al., 2016
	4723	OFCEAS	DFB	298-323	Ventrillard et al., 2015
	4995-5007 (4 pts)	**CRDS**	**DFB**	**297.7**	**This work**
6300 cm^{-1} (1.6 µm)	5875-6665 (10 pts)	CRDS	DFB	302-340	Mondelain et al. 2013; 2014
8000 cm^{-1} (1.25 µm)	7500-7920 (30 pts)	CRDS	DFB	297	Campargue et al., 2016
	7920-8300 (26 pts)	CRDS	ECDL	297	

Note.

[a] QCL: Quantum Cascade Laser, ICL: Interband Cascade Laser, DFB: Distributed Feed Back diode laser, VECSEL: Vertical External Cavity Surface Emitting Laser.

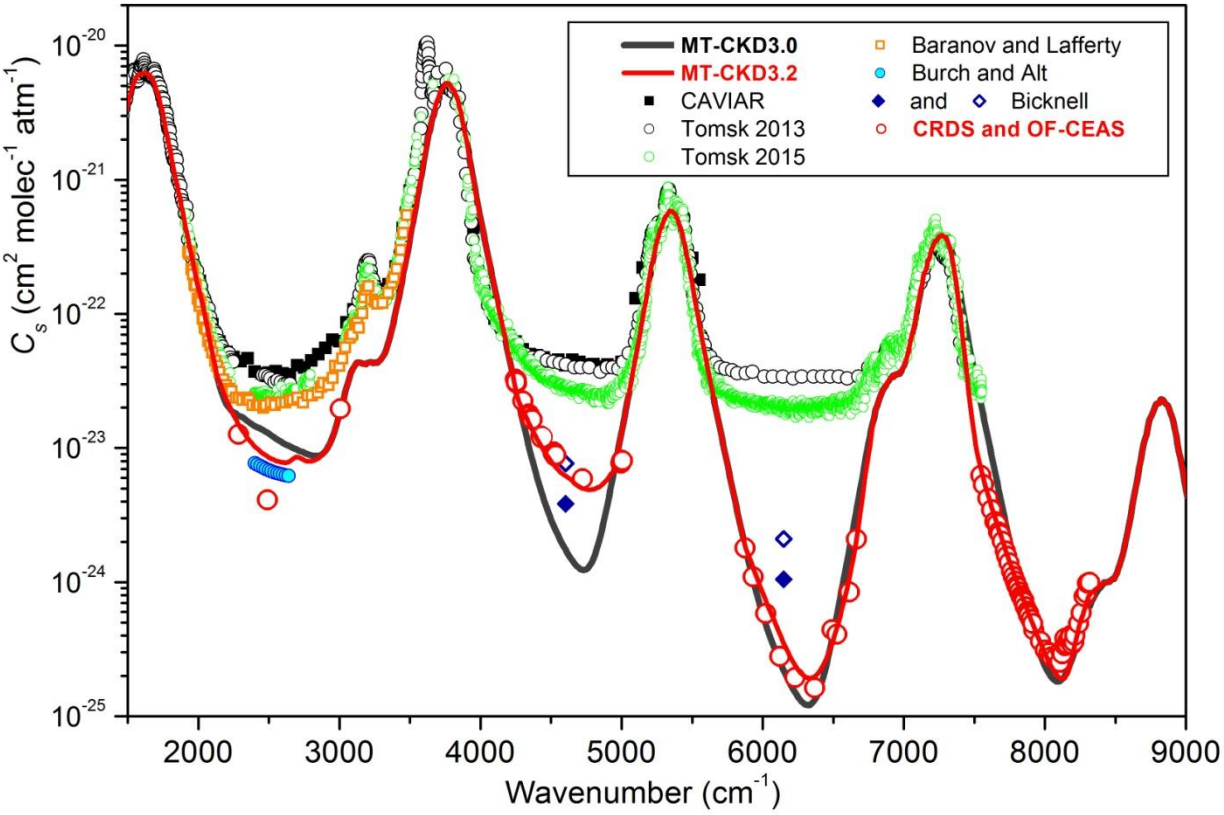

Figure 8: MT_CKD3.0 and 3.2 models (black and red solid lines, respectively) (Mlawer et al. 2012) of the water vapor self-continuum cross-sections, C_S, in the 1500-9000 cm^{-1} range, compared to an exhaustive collection of experimental determinations: *(i)* FTS values reported by Baranov and Lafferty (2011) (orange squares); by the CAVIAR consortium (Ptashnik et al., 2011a) (black full squares), and from Tomsk2013 and Tomsk2015 experiments (Ptashnik et al., 2013, 2015) (black and green open circles, respectively); *(ii)* results by Bicknell et al. (2006) from calorimetric-interferometry in air at 4605 cm^{-1} (blue open diamond corresponds to a measurement in air, blue full diamond is an estimation of the self-continuum contribution) *(iii)* measurements by Burch and Alt (1984) near 2500 cm^{-1} using a grating spectrograph (open blue circles); *(iv)* present and previous measurements by CRDS and OFCEAS (red open circles).

Much laboratory work is still required to characterize the water continuum and fulfill the demands of atmospheric applications. In particular, only very partial information is available concerning the temperature dependence. By complementing OFCEAS results near room temperature with previous high temperature FTS measurements (obtained at higher pressure, thus reliable), the temperature dependence at several spectral points of the 4.0 and 2.1 µm windows was found to follow a simple exp(D_0/kT) dependence, D_0 being the dissociation energy of the water dimer (~1100 cm^{-1}) (Ventrillard et al., 2015; Richard et al. 2017). Let us note that partially resolved absorption features due to water dimers have been identified in the mm-range room-temperature spectrum of water vapor (Tretyakov et al., 2013) and evidence of the water dimer contribution to the continuum was reported in the 14-35 cm^{-1} region (Odintsova et al. 2017) and in the region of

the absorption bands (Paynter et al., 2007; Ptashnik et al., 2008; 2011b). Nevertheless, in the absence of theoretical support, it seems hazardous to consider the exp(D_0/kT) empirical law as an experimental signature of the water dimer origin of the continuum in the studied transparency windows.

In the Earth's atmosphere, the foreign-continuum contribution of the interaction of water molecules with nitrogen and oxygen may be comparable to that of the self-continuum (Mondelain et al. 2015). FTS measurements by Ptashnik et al., 2012 indicated that the foreign continuum in the near-infrared windows was typically between one and two orders of magnitude stronger than that given in previous versions (2.5 and earlier) of the MT_CKD model. In the more recent versions, foreign continuum coefficients were increased in the 4.0 and 2.1 μm windows on the basis of measurements by Baranov and Lafferty (2012), IASI (Alvarado et al., 2013) and Mondelain et al. (2014). We should remark that the quality of the foreign-continuum retrieval from spectra of water in air depends on the accuracy of the self-continuum contribution which has to be subtracted. We have demonstrated that cavity enhanced laser absorption methods provide a powerful approach for an accurate characterization of the self-continuum near room temperature. In the future, we plan to adapt our experimental setups to perform similar studies of the water vapor foreign-continuum.

In recent works, Paynter and Ramaswamy (2011, 2012) constructed an empirical water vapor continuum (BPS-MTCKD continuum) by modifying the MT_CKD model in the near infrared windows mostly according to FTS values of the CAVIAR consortium. They showed that the self- and foreign-water vapor continuum could result in between 1.1 and 3.2 Wm^{-2} additional clear-sky absorption of solar radiation, with this large error bar being due to the "fairly large measurement uncertainties in the shortwave near-infrared window". Ptashnik et al. (2011a) also quantified the impact of the CAVIAR self-continuum cross-sections upon solar radiation absorbed by the atmosphere and obtained a significant additional global mean absorption of ~ 0.75 Wm^{-2} relative to the MT_CKD2.5 i.e. about 1% of the total clear-sky absorption. During very recent years, a set of CRDS and OFCEAS self-continuum cross-sections were obtained over four transparency windows with accuracy as good as a few %. These high sensitive cavity-based measurements dismantled the possibility of the self-continuum in the near-infrared windows being as high as the room-temperature FTS measurements. We hope that these results and the forthcoming studies of the foreign-continuum will help to reduce significantly the uncertainty of the impact of the water continuum on the Earth's clear-sky radiation budget.

Acknowledgements

This project is supported by the LabexOSUG@2020 (ANR10 LABX56) and the LEFE-ChAt program from CNRS-INSU. The research leading to the results at 3.33μm has received funding from the European Community's Seventh Framework Program ERC-2011-AdG under grant agreement n° 291062 (ERC ICE&LASERS), as well as ERC-2015-PoC under grant agreement n° 713619 (ERC OCEAN-IDs).

References

Baranov, Y. I., and Lafferty, W. J.: The water-vapor continuum and selective absorption in the 3-5 μm spectral region at temperatures from 311 to 363 K, J. Quant. Spectrosc. Radiat. Transf., 112, 1304-1313, doi:10.1016/j.jqsrt.2011.01.024, 2011.

Barber, R. J., Tennyson, J., Harris, G. J., Tolchenov, R. N.: A high-accuracy computed line list, Mon. Not. R. Astron. Soc., 368, 1087-94, 2006.

Bicknell, W. E., Cecca, S. D., and Griffin, M. K.: Search for low-absorption regimes in the 1.6 and 2.1 μm atmospheric windows, Journal of Directed Energy, 2, 151-161, 2006.

Burch, D. E.: Continuum absorption by H_2O. Report AFGL-TR-81-0300, Air Force Geophys. Laboratory, Hanscom AFB, MA, 1982.

Burch, D. E., and Alt, R. L.: Continuum absorption by H_2O in the 700 – 1200 cm^{-1} and 2400 – 2800 cm^{-1} windows, Report AFGL-TR-84-0128, Air Force Geophys. Laboratory, Hanscom AFB, MA., 1984.

Burch, D. E.: Absorption by H_2O in narrow windows between 3000 and 4200 cm^{-1}, Report AFGL-TR-85-0036, Air Force Geophys. Laboratory, Hanscom AFB, MA., 1985.

Buryak, I., Vigasin, A. A.: Classical calculation of the equilibrium constants for true bound dimers using complete potential energy surface, J. Chem.Phys., 143, 234304, 2015.

Campargue, A., Kassi, S., Mondelain, D., Vasilchenko, S., Romanini, D., Accurate laboratory determination of the near infrared water vapor self-continuum: A test of the MT_CKD model, J. Geophys. Res. Atmos., 121, 13, 180 – 13,203, doi:10.1002/2016JD025531, 2016.

Campargue, A.,Mikhailenko, S.N., Vasilchenko, S., Reynaud, C., Béguier, S., Čermák, P., Mondelain, D., Kassi, S., Romanini, D.: The absorption spectrum of water vapor in the 2.2 μm transparency window: high sensitivity measurements and spectroscopic database, J. Quant. Spectrosc. Radiat. Transf., 189 407–416.10.1016/j.jqsrt.2016.12.016, 2017.

Camy-Peyret, C., Vigasin, A. A. (Eds).: Weakly Interacting Molecular Pairs: Unconventional Absorbers of Radiation in the Atmosphere. NATO ARW Proceedings Series, Kluwer, Dordrecht, 2003.

Čermák, P., Chomet, B., Ferrieres, L., Vasilchenko, S., Mondelain, D., Kassi, S., et al.: CRDS with a VECSEL for broad-band high sensitivity spectroscopy in the 2.3μm window, Rev. Sci. Instrum., 87(8):083109. doi:10.1063/1.4960769, 2016.

Clough, S. A., Kneizys, F. X., and Davies, R. W.: Line shape and the water vapor continuum, Atmospheric Research, 23, 229-241, doi:10.1016/0169-8095(89)90020-3, 1989.

Desbois, T., Ventrillard I., and Romanini D.: Simultaneouscavity-enhanced and cavityringdown absorption spectroscopyusingoptical feedback, Appl. Phys., B 116: 195–201. doi:10.1007/s00340-013-5675-z, 2014.

Faïn, X., Chappellaz, J., Rhodes, R. H., Stowasser, C., Blunier, T., McConnell, J. R., Brook, E. J., Preunkert, S., Legrand, M., Debois, T., and Romanini, D.: High resolution measurements of carbon monoxide along a late Holocene Greenland ice core: evidence for in situ production, Clim. Past., 10, 987-1000, doi:10.5194/cp-10-987-2014, 2014.

Forget, F., Leconte, J.: Possible climates on terrestrial exoplanets, Phil Trans R Soc A, 372, 20130084, 2014.

Gagliardi, G., Loock, H. P.: (Eds.). Cavity-enhanced spectroscopy and sensing, Springer, London, UK, 2014.

Gordon, I. E., Rothman, L. S., Hill, C., Kochanov, R. V., Tan, Y., Bernath, P. F., Birk, M., Boudon, V., Campargue, A., Chance, K. V., Drouin, B. J., Flaud, J. M., Gamache, R. R., Hodges, J. T., Jacquemart, D., Perevalov, V. I., Perrin, A., Shine, K. P., Smith, M. A. H., Tennyson, J., Toon, G. C., Tran, H., Tyuterev, V. G., Barbe, A., Császár, A. G., Devi, V. M., Furtenbacher, T., Harrison, J. J., Hartmann, J. M., Jolly, A., Johnson, T. J., Karman, T., Kleiner, I., Kyuberis, A. A., Loos, J., Lyulin, O. M., Massie, S. T., Mikhailenko, S. N., Moazzen-Ahmadi, N., Müller, H. S. P., Naumenko, O. V., Nikitin, A. V., Polyansky, O. L., Rey, M., Rotger, M., Sharpe, S. W., Sung, K., Starikova, E., Tashkun, S. A., Vander Auwera, J., Wagner, G., Wilzewski, J., Wcisło, P., Yu, S., Zak, E. J.: The HITRAN2016 Molecular Spectroscopic Database, J. Quant. Spectrosc. Radiat. Transf., 203, 3-69, 2017.

Held, I. M., and Soden, B. J.: Water vapor feedback and global warming, Annu. Rev. Energy Environ., 25, 441–475, doi:10.1146/annurev.energy.25.1.441, 2000.

Jacquinet-Husson, N., Armante, R., Scott, NA., Chédin, A., Crépeau, L., Boutammine, C., Bouhdaoui, A., Crevoisier, C., Capelle, V., Boonne, C., Poulet-Crovisier, N., Barbe, A., Benner, D. C., Boudon, V., Brown, L. R., Buldyreva, J., Campargue, A., Coudert, L. H., Devi, V. M., Down, M. J., Drouin, B. J., Fayt, A., Fittschen, C., Flaud, J. M., Gamache, R. R., Harrison, J. J., Hill, C., Hodnebrog, Ø., Hu, S. M., Jacquemart, D., Jolly, A., Jiménez, E., Lavrentieva, N. N., Liu, A. W.,

Lodi, L., Lyulin, O. M., Massie, S. T., Mikhailenko, S., Müller, H. S. P., Naumenko, O. V., Nikitin, A., Nielsen, C. J., Orphal, J., Perevalov, V. I., Perrin, A., Polovtseva, E., Predoi-Cross, A., Rotger, M., Ruth, A. A., Yu, S. S., Sung, K., Tashkun, S. A., Tennyson, J., Tyuterev, V. G., Vander Auwera, J., Voronin, B. A., Makie, A.: The 2015 edition of the GEISA spectroscopic database, J. Mol.Spectrosc., 327, 31-72, 2016.

Kassi, S., Chenevier, M., Gianfrani, L., Salhi, A., Rouillard, Y., Ouvrard, A. and Romanini, D.: Looking into the volcano with a Mid-IR DFB diode laser and Cavity Enhanced Absorption Spectroscopy, Opt. Express, 14, 11442-11452, doi: 10.1364/OE.14.011442, 2006.

Kasting, J., Whitmire, D. P., Reynolds, R. T.: Habitable zones around main sequence stars, Icarus, 101, 108-28, 1993.

Kerstel, E., Iannone, R. Q., Chenevier, M., Kassi, S., Jost, H. J., and Romanini, D.: A water isotope (^{2}H, ^{17}O, and ^{18}O) spectrometer based on optical feedback cavity-enhanced absorption for in situ airborne applications, Applied Physics B-Lasers and Optics, 85, 397-406. doi:10.1007/s00340-006-2356-1, 2006.

Kopparapu, R. K., Ramirez, R., Kasting, J. F., Eymet, V., Robinson, Mahadevan, S., Terrien, R. C., Domagal-Goldman, S., Meadows, V. and Deshpande, R.: Habitable zone around the main sequence stars: new estimates, Astrophysical Journal, 765, 131, doi:10.1088/0004-637X/765/2/131, 2013.

Leconte, J., Forget, F., Charnay, B., Wordsworth, R., Pottier, A.: Increased insolation threshold for runaway greenhouse processes on Earth-like planets, Nature, 504, 268, doi:10.1038/nature12827, 2013a.

Leconte, J., Forget, F., Charnay, B., Wordsworth, R., Selsis, F., Millour, E., Spiga, A.: 3D climate modeling of close-in land planets: circulation patterns, climate moist bistability, and habitability, Astron. Astrophys., 554, A69, doi:10.1051/0004-6361/201321042, 2013b.

Leforestier, C., Tipping, R. H., Ma, Q.: Temperature dependences of mechanisms responsible for the water-vapor continuum absorption. II. Dimers and collision-induced absorption, J. Chem.Phys., 132, 164302, 2010.

Lin,Q., VanCamp,M. A., Zhang,H., Jelenković, B., Vuletić,V.: Long-external-cavity distributed Bragg reflector laser with subkilohertz intrinsic linewidth. Opt Lett., 37:1989-91. doi:10.1364/OL.37.001989, 2012.

Loos, J., Birk, M., Wagner, G.: Measurement of air-broadening line shape parameters and temperature dependence parameters of H_2O lines in the spectral ranges 1850–2280cm^{-1} and 2390–4000cm^{-1}, J. Quant. Spectrosc. Radiat. Transf., 203, 103-118, doi:10.1016/j.jqsrt.2017.03.033, 2017.

Ma, Q., Tipping, R. H., Leforestier, C.: Temperature dependences of mechanisms responsible for the water-vapor continuum absorption. I. Far wings of allowed lines, J. Chem.Phys., 128, 124313, 2008.

Maisons, G., Gorrotxategi-Carbajo, P., Carras, M. and Romanini, D.: Optical-feedback cavity-enhanced absorption spectroscopy with a quantum cascade laser, Opt. Lett., 35, 3607–3609, doi: 10.1364/OL.35.003607, 2010.

Mlawer, E. J., Payne V. H., Moncet, J., Delamere, J. S., Alvarado, M. J. and Tobin, D.C.: Development and recent evaluation of the MT_CKD model of continuum absorption, Phil. Trans. R. Soc. A, 370, 2520–2556, doi:10.1098/rsta.2011.0295, 2012.

Mondelain, D., Aradj, A., Kassi, S. and Campargue, A.: The water vapour self-continuum by CRDS at room temperature in the 1.6 μm transparency window, J. Quant. Spectrosc. Radiat. Transf., 130, 381-391. doi:10.1016/j.jqsrt.2013.07.006, 2013.

Mondelain, D., Manigand, S., Manigand, S., Kassi, S., and Campargue, A.: Temperature dependence of the water vapor self-continuum by cavity ring-down spectroscopy in the 1.6 μm transparency window, J. Geophys. Res. Atmos., 119, 9, 2169-8996, doi:10.1002/2013JD021319, 2014.

Mondelain, D., Vasilchenko, S., Cermak, P., Kassi, S., and Campargue, A.: The self- and foreign-absorption continua of water vapor by cavity ring-down spectroscopy near 2.35 μm, Phys. Chem. Chem. Phys., 17, 27, 17762-1777, 35 doi:10.1039/C5CP01238D, 2015.

Mondelain, D., Vasilchenko, S., Čermák, P., Kassi, S., Campargue, A.: The CO_2 absorption spectrum in the 2.3μm transparency window by high sensitivity CRDS: (II) Self absorption continuum, J. Quant. Spectrosc. Radiat. Transf.,187, 38-43. doi:10.1016/j.jqsrt.2016.09.003., 2017.

Morville, J., Romanini, D., Kachanov, A. A., Chenevier M.: Two schemes for trace detection using cavity ringdown spectroscopy, Appl. Phys., 78, 465–476, doi:10.1007/s00340-003-1363-8, 2004.

Odintsova, T. A., Tretyakov, M. Y., Pirali, O., Roy, P.: Water vapor continuum in the range of rotational spectrum of H_2O molecule: New experimental data and their comparative analysis, J. Quant. Spectrosc. Radiat. Transf., 187, 116-23, 2017.

Paynter, D. J., Ptashnik, I. V., Shine, K. P., Smith, Pure water vapor continuum measurements between 3100 and 4400 cm^{-1}: Evidence for water dimer absorption in near atmospheric conditions, Geophys. Res. Let., 34, L12808, doi:10.1029/2007GL029259, 2007.

Paynter, D. J. and Ramaswamy, V.: An assessment of recent water vapor continuum measurements upon longwave and shortwave radiative transfer, J. Geophys. Res., 116, D20302, doi:10.1029/2010JD015505, 2011.

Paynter, D. J., and Ramaswamy, V.: Variations in water vapor continuum radiative transfer with atmospheric conditions, J. Geophys. Res., 117, D16310, doi:10.1029/2012JD017504, 2012.

Paynter, D. J. and Ramaswamy, V.: Investigating the impact of the shortwave water vapor continuum upon climate simulations using GFDL global models, J. Geophys. Res. Atmos., 119, 10, 720–10, 737, doi:10.1002/2014JD021881, 2014.

Paynter, D. J., Ptashnik, I. V., Shine, K. P., Smith, K. M., McPheat, R., and Williams, R. G.: Laboratory measurements of the water vapor continuum in the 1200–8000 cm^{-1} region between 293 K and 351 K, J. Geophys. Res., 114, D21301, doi:10.1029/2008JD011355, 2009.

Ptashnik, I. V., McPheat, R. A., Shine, K. P., Smith, K. M., and Williams, R. G.: Water vapor self - continuum absorption in near - infrared windows derived from laboratory measurements, J. Geophys. Res., 116, D16305, doi:10.1029/2011JD015603, 2011a.

Ptashnik, I. V., Shine, K. P., Vigasin, A. A.: Water vapour self-continuum and water dimers: 1. Analysis of recent work, J Quant. Spectrosc. Radiat. Transf., 112, 1286-303, 2011b.

Ptashnik, I. V., McPheat, R. A., Shine, K. P., Smith, K. M., and Williams, R. G.: Water vapour foreign-continuum absorption in near-infrared windows from laboratory measurements, Philosophical Transactions of the Royal Society a-Mathematical Physical and Engineering Sciences, 370, 2557-2577, doi:10.1098/rsta.2011.0218, 2012.

Ptashnik, I. V., Petrova, T. M., Ponomarev, Y. N., Shine, K. P., Solodov, A. A., and Solodov, A. M.: Near-infrared water vapour self-continuum at close to room temperature, J. Quant. Spectrosc. Radiat. Transf., 120, 23-35, doi:10.1016/j.jqsrt.2013.02.016, 2013.

Ptashnik, I. V., Petrova, T. M., Ponomarev, Y. N., Solodov, A. A., and Solodov, A. M.: Water vapor continuum absorption in near-IR atmospheric windows, Atmospheric and Oceanic Optics, 28, 115 – 120, doi:10.1134/S102485601502009, 2015.

Ptashnik, I. V.: Evidence for the contribution of water dimers to the near-IR water vapour self-continuum, J Quant Spectrosc. Radiat. Transf., 109, 831-52, 2008.

Richard, L., Vasilchenko, S., Mondelain, D., Ventrillard, I, Romanini, D., Campargue, A.: Water vapor self-continuum absorption measurements in the 4.0 and 2.1 μm transparency windows, J Quant. Spectrosc. Radiat. Transf., 201, 171-9, 2017.

Rocher-Casterline, B. E.,Ch'ng,L. C.,Mollner,A. K. AndReisler,H.: Determination of the bond dissociation energy (D_0) of the water dimer, $(H_2O)_2$, by velocity map imaging, Chem, J.:Phys., 134, 211101, 2011.

Romanini, D., Chenevier, M., Kassi, S., Schmidt, M., Valant, C., Ramonet, M., Lopez, J., and Jost, H. J.: Optical-feedback cavity-enhanced absorption: a compact spectrometer for real-time measurement of atmospheric methane, App. Phys. B-Lasers and Optics., 83, 659-667, doi:10.1007/s00340-006-2177-2, 2006.

Rubens, H., Aschkinass, E.: Beobachtungenüber Absorption und Emission von Wasserdampf und Kohlensaüreimultrarothen Spectrum, Ann. Phys., 300, 584–601, 1898.

Schwenke, D. W., Partridge, H.: Convergence testing of the analytic representation of an *ab initio* dipole moment function for water: Improved fitting yields improved intensities, J. Chem. Phys., 113:6592-7, 2000.

Serov, E. A., Odintsova, T. A., Tretyakov, M. Y., Semenov, V. E.: On the origin of the water vapor continuum absorption within rotational and fundamental vibrational bands. J. Quant. Spectrosc. Radiat. Transf., 193, 1-12, 2017.

Shine, K. P., Ptashnik, I. V., and Rädel, G.: The Water Vapour Continuum: Brief History and Recent Developments, Surv. Geophys., 33, 535–555, doi:10.1007/s10712-011-9170-y, 2012.

Shine, K. P., Campargue, A., Mondelain, D., McPheat, R. A., Ptashnik, I. V., and Weidmann D.: The water vapour continuum in near-infrared windows – current understanding and prospects for its inclusion in spectroscopic databases, J. Mol. Spectrosc., 327, 193–208, doi:10.1016/j.jms.2016.04.011, 2016.

Thalman, R., Zarzana, K., Tolbert, M. A., and Volkamer, R.: Rayleigh scattering cross-section measurements of nitrogen, argon, oxygen and air, J. Quant. Spectrosc. Radiat. Transf., 147, 171–177, doi:10.1016/j.jqsrt.2014.05.030, 2014,

Tretyakov, M. N., Serov, E. A., Koshelev, M. A., Parshin, V. V., Krupnov, A. F.: Water dimer rotationally resolved millimeter-wave spectrum observation at room temperature, Phys. Rev. Lett., 110, 093001, 2013.

Tretyakov, M. Y., Koshelev, M. A., Serov, E. A., Parshin, V. V., Odintsova, T. A., Bubnov, G. M.: Water dimer and the atmospheric continuum. UspekhiFizNauk, 184, 1199-215 (in Russian). English translation available in Physics - Uspekhi, 57, 1083-98, 2014.

Ventrillard, I., Romanini, D., Mondelain, D., and Campargue, A.: Accurate measurements and temperature dependence of the water vapor self-continuum absorption in the 2.1 μm atmospheric window, J. Chem.Phy., 143, doi:10.1063/1.4931811, 2015.

Vigasin, A. A.: Water vapor continuum: Whether collision-induced absorption is involved? J. Quant.Spectrosc. Radiat. Transf., 148, 58-64, 2014.